Measurement of stiffness of tress stems using acoustic velocity measurements made across the stem

Mathew Legg
Physics Department, University of Auckland, Auckland, New Zealand, m.legg@auckland.ac.nz

Stuart Bradley
Physics Department, University of Auckland, Auckland, New Zealand, s.bradley@auckland.ac.nz

Abstract

Standing tree stiffness measurements are commonly calculated using acoustic Time of Flight (TOF) velocity measurements. These are generally obtained by measuring the propagation time of an acoustic signal between two probes inserted into the “same face” of the tree. Studies have suggested that these TOF measurements are biased to measure the outerwood stiffness rather than that of the tree stem as a whole. However, the stiffness of tree stems increase from pith to bark. In this paper, a technique is investigated, which uses TOF measurements on the "opposite faces" of the tree stem to attempt to obtain an average stiffness through the tree stem. Unlike previous studies, this technique allows for the anisotropic nature of wave propagation in wood. The measured Modulus of Elasticity (MOE) values are compared to MOE values obtained using the "same face" TOF and acoustic resonance techniques.

Keywords: stiffness, time of flight, opposite face, anisotropic

Introduction

The stiffness of wood is related to the Modulus of Elasticity (MOE), or Young's E modulus, of the wood. Bending tests can be used to measure the static modulus of elasticity. However, these are generally destructive tests. Acoustic nondestructive testing (NDT) techniques have, therefore, been developed to measure the dynamic modulus of elasticity *E*. This is calculated using

$$E = \rho c^2 \tag{1}$$

where c is the acoustic wave velocity in the longitudinal direction, see Figure 1, and ρ is mass density of material (Ross and Pellerin, 1994). For logs, the velocity is usually measured using acoustic resonance. The end of the log is hit with a hammer and the signal is recorded and the spectrum obtained. The resonance acoustic velocity is then calculated for the n^{th} resonance frequency f_n using

$$c_{RES} = \frac{2Lf_n}{n}, \tag{2}$$

where *L* was the length of the log. Resonance techniques have been reported to give stiffness measurements that compare well with static MOE values obtained using bending tests (Harris, Petherick and Andrews, 2002). Different resonance harmonics may generate different results. According to Chauhan and Walker (2006), the second harmonic appears to be that used by the commercial resonance tool Hitman[1].

[1] http://www.fibre-gen.com

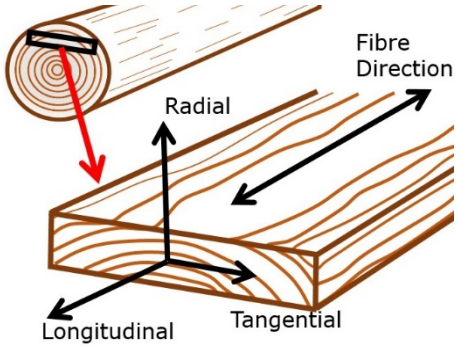

Figure 1: Diagram illustraiting the longitudinal, radial, and tangential orthotropic axis directions for wood.

Resonance cannot be used for standing trees. Instead the stiffness is measured using TOF techniques (Wang et al., 2001). These measurements are generally obtained by inserting two probes into a tree stem on the "same face" of the tree, separated vertically by a distance *z*, usually about a meter, see Figure 2(a). The acoustic velocity is calculated from the acoustic propagation time *T* between the two probes using

$$c_{TOF} = \frac{z}{T}, \tag{3}$$

The TOF is measured by detecting the start time of the signal. TOF techniques have been reported to provide stiffness measurements that are higher than those obtained using resonance or bending tests (Wang, Ross and Carter, 2007). This has been suggested to be due to the increase in stiffness and hence acoustic velocity in tree stems from pith to bark (Hsu, 2003; Wang et al., 2004; Chauhan and Walker, 2006; Lasserre, Mason and Watt, 2007). An alternative explanation is that the TOF method measures a "dilation speed", while the resonance measures the "rod speed" (Andrews, 2002; Wang, 2013).

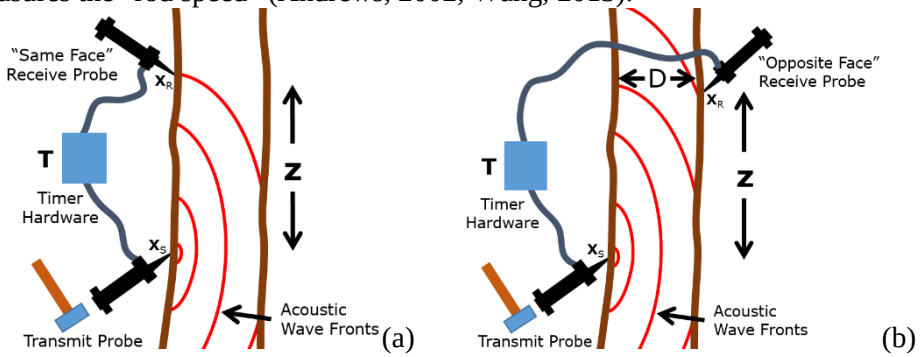

Figure 2: Diagrams illustrating time of flight velocity measurements made using (a) "same face" and (b) "opposite face" techniques.

There has been results which suggest that "same face" TOF stiffness measurements are more closely correlated to with outerwood stiffness (Grabianowski, Manley and Walker, 2006; Mora et al., 2009). To try to compensate for this, some studies have been made TOF measurements on "opposite faces" of the tree with the probes separated vertically by about a meter, see Figure 2(b) (Joe et al., 2004; Mahon et al., 2009; Matheson et al., 2002; Dickson, Raymond, Joe and Wilkinson, 2003; Dickson et al., 2004; Mahon, 2007). However, none of these studies have allowed for the anisotropic nature of wood, where the velocity in the radial direction is significantly less than that in the longitudinal direction. This resulted in stiffness measurements that were too low. Also, most have not included the true propagation path distance in the TOF velocity measurements, which has resulted in stiffness measurements that varied with the diameter of the tree stem. This means that the longitudinal velocity cannot be calculated using Equation (3).

In order for the "opposite face" method to be used for longitudinal velocity measurements, a model of the anisotropic wave propagation in tree stems needs to be obtained for the longitudinal-radial plane. Acoustic

TOF measurements in logs have been presented in references (Zhang, Wang and Su, 2011; Zhang, Wang and Ross, 2009; Su, Zhang and Wang, 2009), though wave propagation models were not provided. Searles (2012) analyzed the data provided by Zhang, Wang and Su (2011) and suggested the wave fronts in the longitudinal-radial plane could be explained by elliptical velocities with the ellipse axes being the longitudinal and radial velocities. Anisotropic wave propagation models in the radial-tangential plane have been investigated in references (Dikrallah et al., 2006; Maurer et al., 2006; Li et al., 2014) for 2D tomography corrections. Maurer et al. (2006) provided a model which was a first order approximation of an ellipse. An 3D anisotropic model may be derived from Kelvin-Christoffel equation (Carcione, 2007a; Bucur, 2006). However, papers verifying this model experimentally for tree stems were not found in the literature.

In this paper, “same face” and “opposite face” techniques are investigated using multi-path TOF measurements. The “opposite face” data is analyzed and a propagation model is presented, which attempts fit the measurements for this log. This model includes the anisotropic nature of wave propagation in wood and the propagation distance. Longitudinal acoustic velocity values obtained using this techniques are compared the “same face” technique and acoustic resonance.

Radiata Pine Log

Acoustic velocity measurements were made in the Acoustics Lab of the Physics Department, the University of Auckland. Measurements were made on a 2.5 meter long radiate pine log, see Figure 3. The diameter of the log at the thin and thick ends of the log was respectively 290 and 340 mm. At the time of measurements, the log had been in the lab for several month and was relatively dry. The transducers were attached directly to surface of log, with the bark removed in the area where the transducers were attached.

Figure 3: Photo log used for measurements with a transducer attached to the surface of the log using a strap.

Resonance Measurements

Acoustic resonance measurements were made for the log. This involved hitting the end of the log with a hammer and recording the resulting signal using a low noise Gras microphone and a Data Translation DT9836 board. A fast Fourier transform of this signal was obtained and the frequencies at which the spectral peaks occurred were measured. Spectral peaks at 566 and 1067 kHz were obtained. Equation (2) was used to obtain the first and second harmonic resonance velocities of 2830 and 2670 m/s. The average of these two is 2750 m/s.

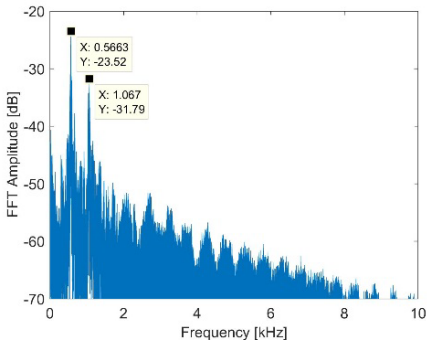

Figure 4: Spectrum for a hammer hit on the end of the log recorded using a microphone. Resonance peaks can be seen at frequencies f_n of 566 and 1067 Hz.

Time of Flight Measurements

Acoustic excitation and reception was made using custom built hardware/software. The excitation signal used was 20 cycles of a Maxim Length Sequence (MLS). This is a series of digital high and low values which has a wide, flat frequency response (0 to 112.5 kHz in this case). These signals were generated using MatLab and played using the analog output of a Data Translation DT9836 board using a sampling rate of 225 kHz. This was amplified to about 250 V_{pp} using a MOSFET/step-up transformer power amplifier (Svilainis and Motiejunas, 2006) and used to drive a shear wave transducer. The resulting signal was measured using one or more shear transducers. This signal was amplified using preamplifier circuits and sampled using an analog input channel of the DT9836 using a sampling rate of 225 kHz.

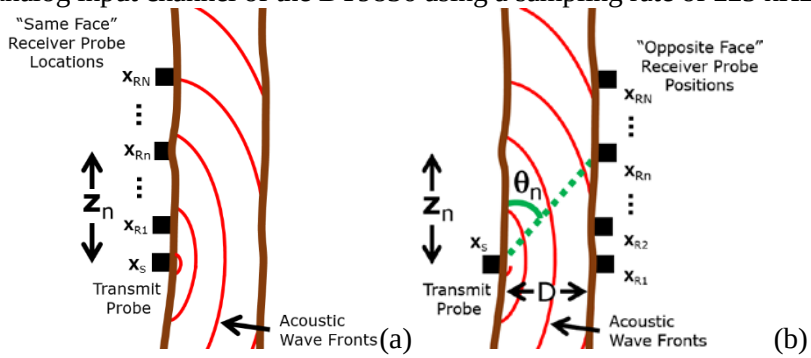

Figure 5: Diagrams showing (a) "same face" and (b) "opposite face" multi-path TOF measurement locations.

The transducers were oriented to excite vibration in the longitudinal direction. The transmit transducer was kept a one location while the receive transducer was move to multiple locations on the log, see Figure 5. The first arrival time *T* of acoustic signal were calculated using an AIC algorithm Picker (Zhang, Thurber and Rowe, 2003).

Same Face Measurements

"Same face" measurements were made at the thin end of the log. The transmit transducer was kept stationary while the receiver transducer was moved incrementally along the log in steps of 50 mm, see Figure 5(a). Example plots of the raw data and AIC picker algorithm output can be seen in Figure 6. With increase propagation distance, the signal was increasingly attenuated. It also appeared that higher frequency components of the signal were increasingly filtered out with propagation distance.

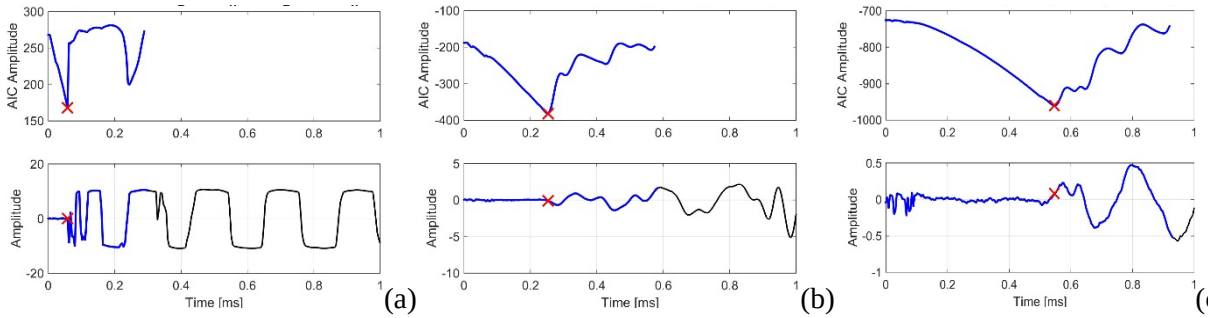

Figure 6: Example plots of raw data (lower) and AIC picker output (upper) for "same face" measurements made at distance z_n of (a) 300, (b) 550, and (c) 800 mm. The first arrival time obtained by the AIC picker is shown in red.

The calculated TOF values were plotted as a function of distance, see Figure 7. It can be seen that the data appears to lie on three straight lines. The sudden jumps may be due to the AIC picker algorithm triggering on different parts of the received signal due to attenuation. Therefore, velocities were calculated using the slope of a least squared fitted line through the data. Three velocities were 4490, 3120, and 3150 m/s were obtained. It appears that the signal initially propagates at a higher velocity (4490 m/s) but subsequently drops to a lower velocity (3120 or 3150 m/s). Potentially the two different velocities could be related a different frequencies components propagating at different velocities but experiencing different attenuation rates. As expected, both these velocities values are higher than that obtained using resonance. The lower of the two velocities is greater by 1.14.

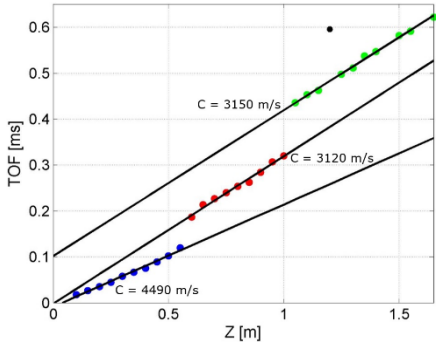

Figure 7: "Same face" AIC time of flight measurements at increamental positions along log. The velocity c is measured using the slope of a fitted line through data points. The two in TOF at about 1 meter appears to be caused by in the AIC picker triggering on a different parts of the received signal.

Opposite Face Measurements

"Opposite face" TOF measurements were also made on the thin end of the log. The transmit transducer was kept stationary, while the receive transducer was moved along the opposite side of the log in steps of 50 mm, see Figure 5(a). The TOF measurements were plotted as a function of distance z_n, see Figure 8(a). It was observed that the data points initially followed a curve but jumped to a higher level after 1050mm. This jump may be caused by the AIC picker algorithm triggering on different parts of the received signal due to attenuation. Velocities were calculated using the measured time of flights T_n and propagation distance R_n

$$c_n = \frac{R_n}{T_n} = \frac{\sqrt{D^2 + z_n^2}}{T_n}. \tag{5}$$

These velocities were analysed and plotted as a function of different parameters. It was observed that the measured velocity data points formed a relatively straight line when plotted as a function of the sin of the angle

$$\sin(\theta) = \frac{D}{\sqrt{D^2 + z_n}}, \tag{6}$$

see Figure 8(b). This indicates that the velocity could be described as

$$c = b - a\sin(\theta), \tag{7}$$

where parameters *a* and b can be obtained from a least squares fit. Taking the limits as the angle θ goes to 0 and 90 degrees, this model suggests that the longitudinal and radial velocities can be obtained from the least squares fitted parameters using

$$c_L = b, \quad c_R = b - a. \tag{8}$$

For the fitted data points, the longitudinal and radial velocities were calculated as 3908 and 1446 m/s respectively. This is higher than that obtained using resonance and the lower of the two velocities obtained using the "same face" technique. Other models, especially one using the Kelvin-Christoffel equation should be investigated.

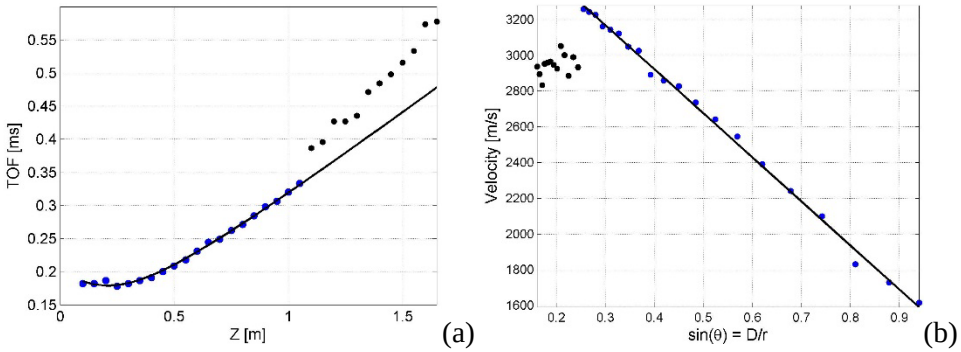

Figure 8: "Opposite face" measured (a) TOF and (b) velocity data points. Overlaid are linear least squared fitted lines. Beyond about a meter, the signal appears to have been attenuated too much for the AIC picker to pick the first arrival time of the signal.

The previous measurement had been made with an impulsive excitation signal using MLS signal and a MOSFET/set-up transformer power amplifier. "Opposite face" measurements were repeated using an arbitrary power amplifier and a transmit signal composed for five cycles of a sine wave (tone burst) and transmit frequencies ranging from 8 to 50 kHz in 0.5 kHz increments. These measurements were made with the transmit receiver both the thin and thick end of the log. The calculated velocities are plotted in Figure 9 as a function of the sin of the angle θ. Relatively similar results were obtained for the different transmit frequencies. However, different lines were obtained for the two ends of the log. This may be related to the thinner end having a lower moisture content than the thicker end and hence higher velocity.

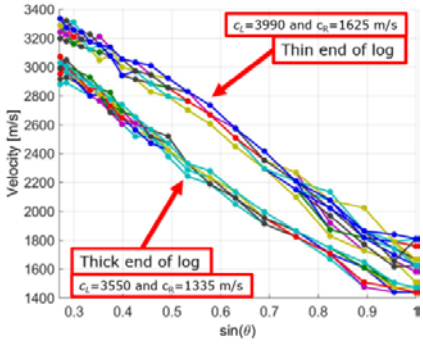

Figure 9: Measured "opposite face" velocities for frequency range of 8 to 50 kHz for two different locations in the log. Estimated values of longitudinal and radial velocities were estimated using Equation (8).

Table 1: Acoustic velocities obtained using different techniques.

Technique	Longitudinal Velocity
Resonance	2830 and 2670 m/s
TOF – "Same Face"	4490, 3120, and 3150 m/s
TOF – "Opposite Face" Model	3550 and 3908 m/s

Conclusions

There have been suggestion in some literature that time of flight measurements made on the same face of the tree tends to provide results that are biased to the outerwood stiffness. Measurements made with the receiver on the opposite face of the stem to the transmitter probe have been proposed as a potential way of obtaining stiffness measurements that are more of an average through the tree stem. However, this technique requires an anisotropic velocity model for the longitudinal-radial plane in order to extract the longitudinal velocity. This paper investigated both the "same face" and "opposite face" techniques using multiple propagation paths TOF measurements. A basic model was presented that explained the "opposite face" measured data for the log being investigated. This provided longitudinal velocities that were higher than those obtained using acoustic resonance and the lower of the two "same face" velocities. This was used with least squares fitting to estimate the longitudinal and radial velocity. Measurements were made using transducers on a log that was relatively dry. More experiments need to be made on standing trees or freshly cut logs to see if similar results are observed. Measurements could also be made using hammer impact on spikes. Also, other models should be investigated, such as that provided by the Kelvin-Christoffel equation.

Acknowledgments

This work was performed as part of the Growing Confidence in Forestry Future project (http://gcff.nz/). Funding was provided through Scion, the New Zealand Ministry of Business, Innovation and Employment and the New Zealand Forest Growers Levy Trust. Authors would like to acknowledge John Moore and Grant Emms of Scion for their help and guidance.

References

Andrews, M., 2002. Which acoustic speed. In: *Proceedings of the 13th International Symposium on Nondestructive Testing of Wood*. pp.159–165.

Bucur, V., 2006. *Acoustics of wood*. 2nd ed. New York: Springer.

Carcione, J.M., 2007a. Anisotropic elastic media. In: *Wave fields in real media: Wave propagation in anisotropic, anelastic, porous and electromagnetic media*. Oxford, Elsevier.

Chauhan, S. and Walker, J., 2006. Variations in acoustic velocity and density with age, and their interrelationships in radiata pine. *Forest Ecology and Management*, 229(1), pp.388–394.

Dickson, R., Matheson, A., Joe, B., Ilic, J. and Owen, J., 2004. Acoustic Segregation of *Pinus radiata* logs for sawmilling. *New Zealand Journal of Forestry Science*, 34(2), pp.175–189.

Dickson, R.L., Raymond, C.A., Joe, W. and Wilkinson, C.A., 2003. Segregation of *Eucalyptus dunnii* logs using acoustics. *Forest Ecology and Management*, 179(1), pp.243–251.

Dikrallah, A., Hakam, A., Kabouchi, B., Brancheriau, L., Baillères, H., Famiri, A. and Ziani, M., 2006. Experimental analysis of acoustic anisotropy of green wood by using guided waves. *Proceedings of the ESWM-COST Action E*, 35, pp.149–154.

Grabianowski, M., Manley, B. and Walker, J., 2006. Acoustic measurements on standing trees, logs and green lumber. *Wood Science and Technology*, 40(3), pp.205–216.

Harris, P., Petherick, R. and Andrews, M., 2002. Acoustic resonance tools. In: *Proceedings, 13th International Symposium on Nondestructive Testing of Wood*. pp.195–201.

Hsu, C.Y., 2003. Radiata pine wood anatomy structure and biophysical properties. PhD thesis, Forestry Department, University of Canterbury, New Zealand.

Joe, B., Dickson, R., Raymond, C., Ilic, J. and Matheson, A., 2004. Prediction of *Eucalyptus Dunnii* and *Pinus Radiata* Timber Stiffness Using Acoustics*: A Report for the RIRDC/Land and Water Australia/FWPRDC/MDBC Joint Venture Agroforestry Program*. RIRDC.

Lasserre, J.-P., Mason, E.G. and Watt, M.S., 2007. Assessing corewood acoustic velocity and modulus of elasticity with two impact based instruments in 11-year-old trees from a clonal-spacing experiment of *Pinus radiata* D. Don. *Forest Ecology and Management*, 239(1), pp.217–221.

Li, G., Wang, X., Feng, H., Wiedenbeck, J. and Ross, R.J., 2014. Analysis of wave velocity patterns in black cherry trees and its effect on internal decay detection. *Computers and Electronics in Agriculture*, 104, pp.32–39.

Mahon, J.M., 2007. The use of acoustics for the wood quality assessment of standing *P. taeda* trees. PhD Thesis. University of Georgia.

Mahon, J.M., Jordan, L., Schimleck, L.R., Clark, A. and Daniels, R.F., 2009. A comparison of sampling methods for a standing tree acoustic device. *Southern Journal of Applied Forestry*, 33(2), pp.62–68.

Matheson, A.C., Dickson, R.L., Spencer, D.J., Joe, B. and Ilic, J., 2002. Acoustic segregation of *Pinus radiata* logs according to stiffness. *Annals of Forest Science*, 59(5-6), pp.471–477.

Maurer, H., Schubert, S.I., Bächle, F., Clauss, S., Gsell, D., Dual, J. and Niemz, P., 2006. A simple anisotropy correction procedure for acoustic wood tomography. *Holzforschung*, 60(5), pp.567–573.

Mora, C.R., Schimleck, L.R., Isik, F., Mahon, J.M., Clark, A. and Daniels, R.F., 2009. Relationships between acoustic variables and different measures of stiffness in standing *Pinus taeda* trees. *Canadian Journal of Forest Research*, 39(8), pp.1421–1429.

Ross, R.J. and Pellerin, R.F., 1994. Nondestructive testing for assessing wood members in structures. *General Technical Report FPL-GTR-70, Forest Products Laboratory, US Department of Agriculture*.

Searles, G., 2012. *Acoustic segregation and structural timber production.* PhD thesis. Edinburgh Napier University.

Su, J., Zhang, H. and Wang, X., 2009. Stress Wave Propagation on Standing Trees-Part 2. Formation of 3D Stress Wave Contour Maps. In: *Series: Conference Proceedings*.

Svilainis, L. and Motiejunas, G., 2006. Power amplifier for ultrasonic transducer excitation. *Ultragarsas*, 1(58), pp.30–36.

Wang, X., 2013. Acoustic measurements on trees and logs: a review and analysis. *Wood Science and Technology*, 47(5), pp.965–975.

Wang, X., Ross, R.J. and Carter, P., 2007. Acoustic evaluation of wood quality in standing trees. Part I. Acoustic wave behavior. *Wood and Fiber Science*, 39(1), pp.28–38.

Wang, X., Ross, R.J., McClellan, M., Barbour, R.J., Erickson, J.R., Forsman, J.W. and McGinnis, G.D., 2001. Nondestructive evaluation of standing trees with a stress wave method. *Wood and Fiber Science*, 33(4), pp.522–533.

Wang, X.R.R.J., Brashaw, B.K., Punches, J., Erickson, J.R., Forsman, J.W. and Pellerin, R.F., 2004. Diameter effect on stress-wave evaluation of modulus of elasticity of logs. *Wood and Fiber Science*, 36(3), pp.368–377.

Zhang, H., Thurber, C. and Rowe, C., 2003. Automatic P-wave arrival detection and picking with multiscale wavelet analysis for single-component recordings. *Bulletin of the Seismological Society of America*, 93(5), pp.1904–1912.

Zhang, H., Wang, X. and Ross, R.J., 2009. Stress wave propagation on standing trees: Part 1. Time-of-flight measurement and 2D stress wave contour maps. In: *16th International Symposium on NDT/NDE of Wood*. Beijing, China, pp.12–14.

Zhang, H., Wang, X. and Su, J., 2011. Experimental investigation of stress wave propagation in standing trees. *Holzforschung*, 65(5), pp.743–748.